

Cell Reports, Volume 25

Supplemental Information

Fasting Imparts a Switch to Alternative

Daily Pathways in Liver and Muscle

Kenichiro Kinouchi, Christophe Magnan, Nicholas Ceglia, Yu Liu, Marlene Cervantes, Nunzia Pastore, Tuong Huynh, Andrea Ballabio, Pierre Baldi, Selma Masri, and Paolo Sassone-Corsi

Figure S1

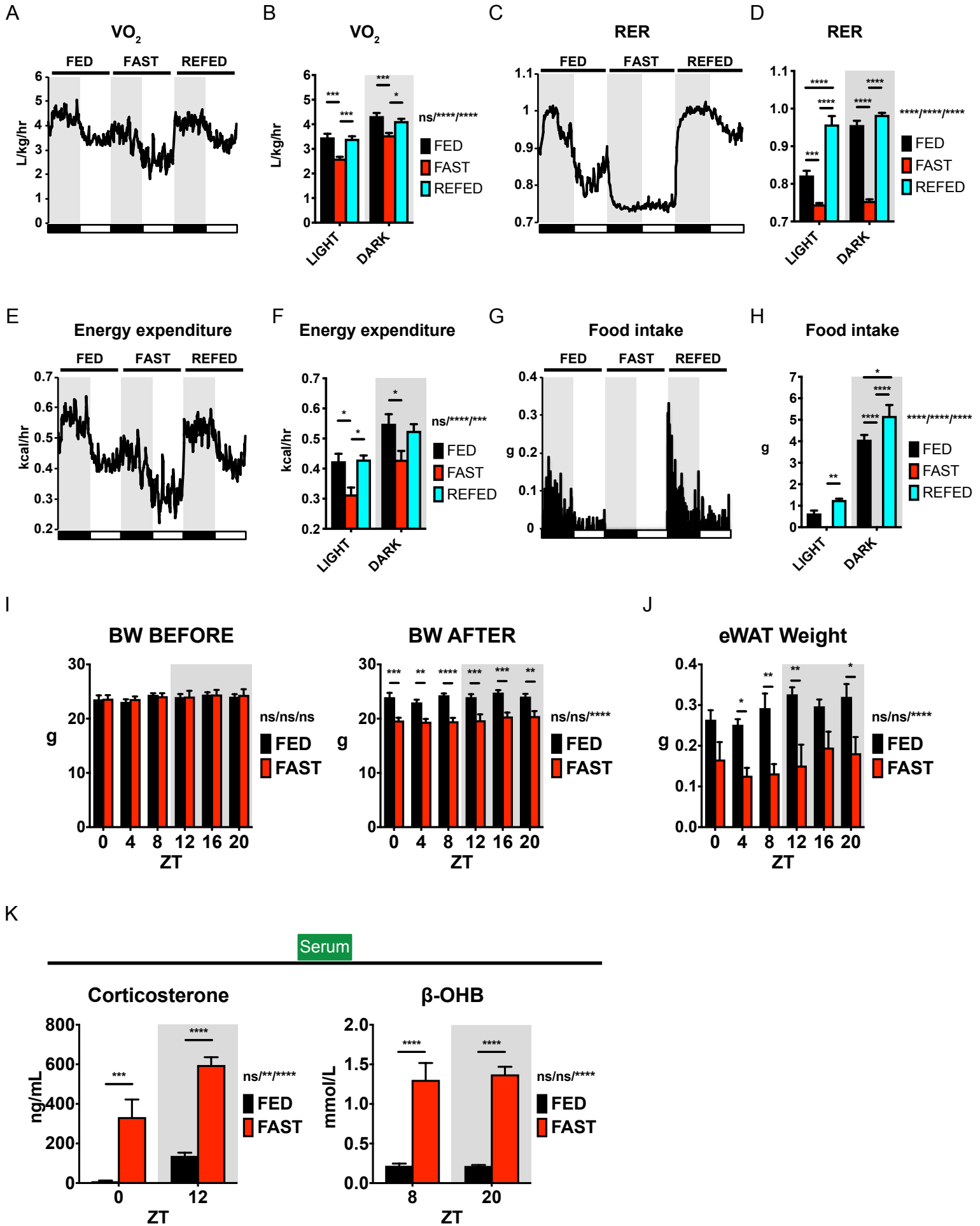


Figure S1. Physical metabolic paradigms after 24-hr fasting and refeeding. Related to Figure 1.

(A and B) Metabolic cage analysis showing measured oxygen consumption (VO_2) for mice under FED, FAST, and REFED conditions and the average during the light and dark phases. (C and D) Metabolic cage analysis showing respiratory exchange ratio (RER) calculated by VCO_2/VO_2 for mice under FED, FAST, and REFED conditions and the average during the light and dark phases. (E and F) Metabolic cage analysis showing energy expenditure for mice under FED, FAST, and REFED conditions and the average during the light and dark phases. (G and H) Metabolic cage analysis showing food intake and the total amount consumed during the light and dark phases. Each parameter was recorded every 10 min over the circadian cycle in wild-type male mice subject to normal chow diet in *ad libitum* for the first 24-hr, subsequently to fasting for 24-hr, and lastly to refeeding for 24-hr. Data are shown as mean for the time series, and as mean + SEM for the average (n=5 biological replicates). (I and J) Body weight of mice before and after 24-hr fasting, and epididymal fat weight after 24-hr fasting at each time point. (K) Serum corticosterone and β -OHB levels from mice under FED and FAST conditions. Data are shown as mean + SEM (n=5 biological replicates per time point per group). * $p < 0.05$, ** $p < 0.01$, *** $p < 0.001$, and **** $p < 0.0001$ by two-way ANOVA (interaction/phase or time/group) with Bonferroni post-hoc tests.

Figure S2

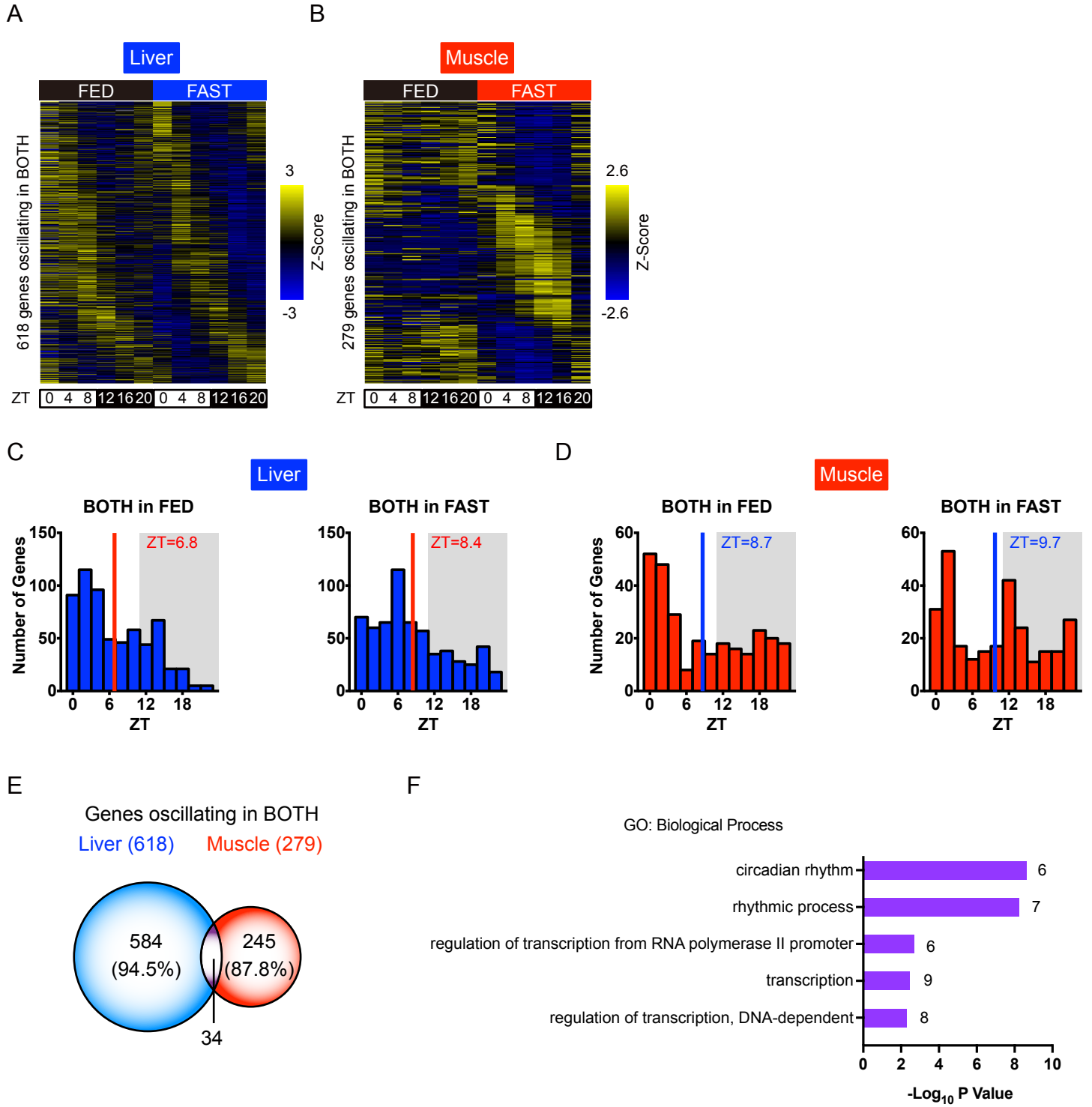


Figure S2. Hepatic and muscle circadian transcriptomes. Related to Figure 1.

(A and B) Heat maps show hepatic and muscle transcripts cycling both in FED and FAST (JTK_CYCLE $P < 0.01$). (C and D) Phase distributions showing the peak phase of hepatic and muscle genes oscillating both in FED and FAST mice. The peak phase in FED is shown on the left panels, and FAST on the right panels. Mean phases are indicated in the graphs. (E) Venn diagrams showing the number of hepatic and muscle cycling transcripts both in FED and FAST. (F) Gene ontology analysis shows top biological processes enriched in rhythmic genes in both FED and FAST in both liver and muscle, with the number of genes indicated on the graph.

Figure S3

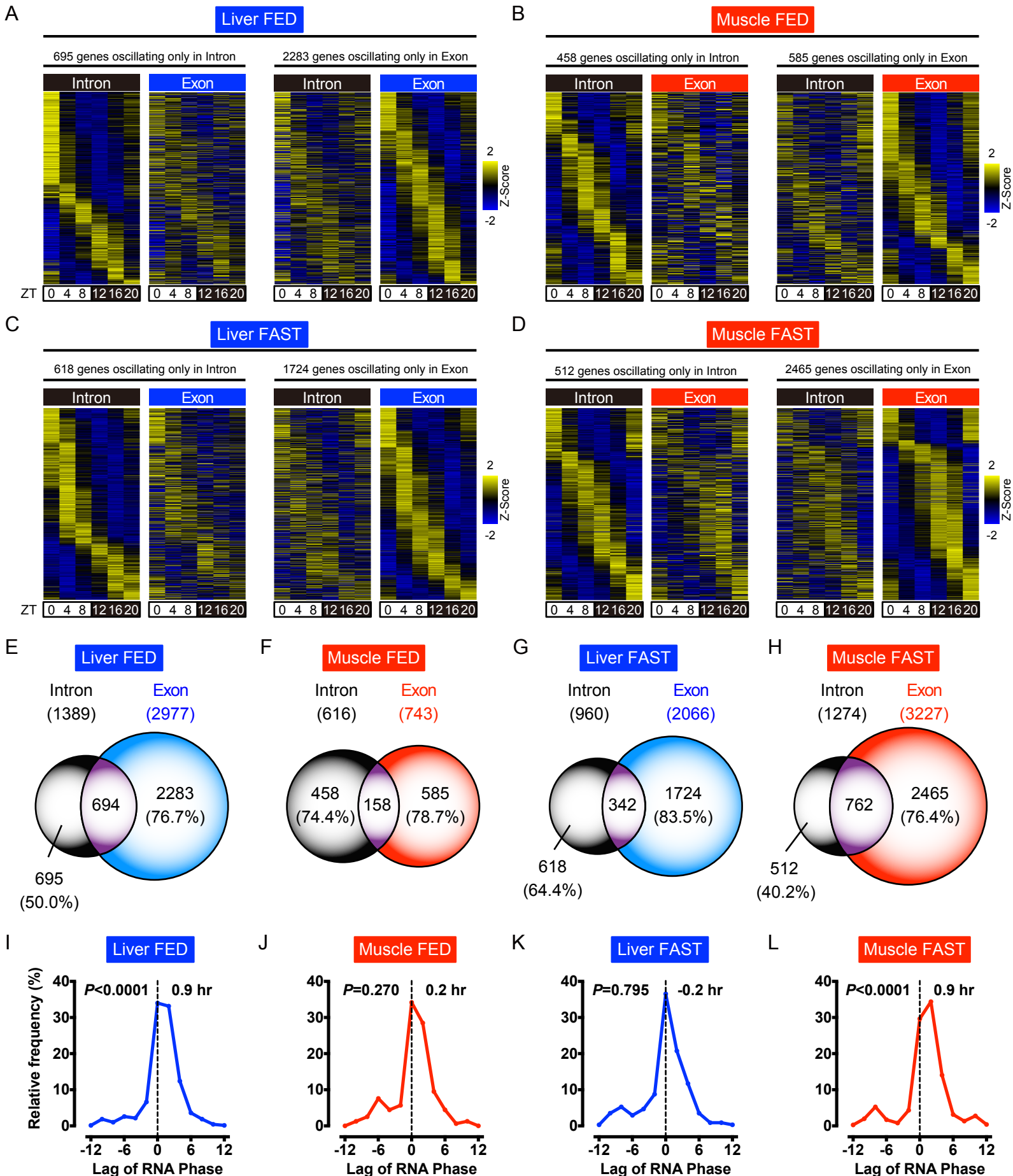
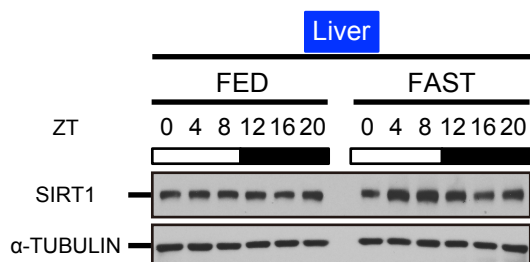


Figure S3. Post-transcriptional control of temporal response to fasting. Related to Figures 1 and 2.

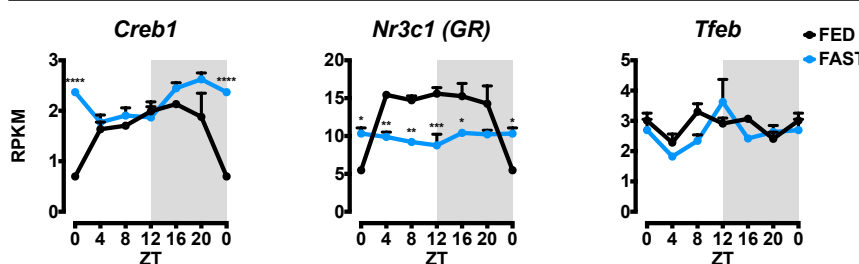
(A-D) Exon Intron Split Analysis was implemented using RNA-seq data from liver and skeletal muscle in FED and FAST conditions. Heat maps show cycling transcripts only in intronic reads (left panels) or in exonic reads (right panels) (JTK_CYCLE $P < 0.01$). (E-H) Venn diagrams indicate the number of oscillating intronic and exonic transcripts in the liver and skeletal muscle in FED and FAST conditions. (I-L) Graphs show the distribution of phase lags of exonic reads compared to intronic reads in the liver and skeletal muscle in FED and FAST conditions. Wilcoxon Signed Rank Test was performed to determine if there is a significant lag compared to theoretical median value (zero).

Figure S4

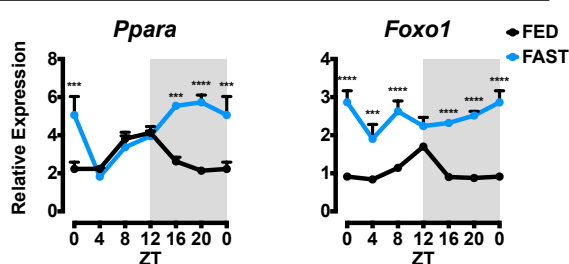
A



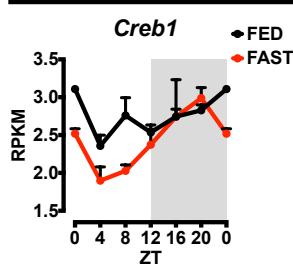
B



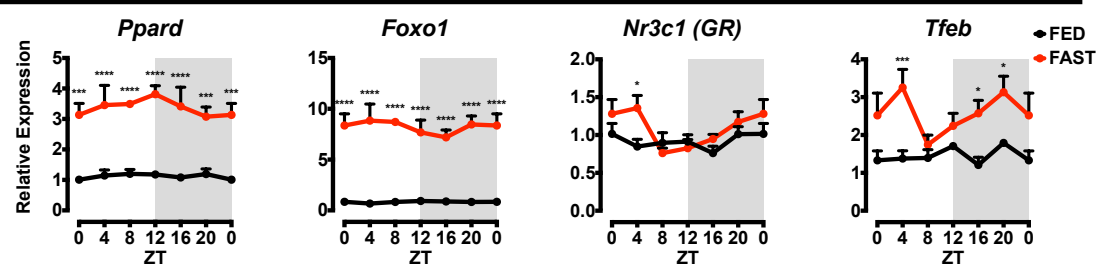
D



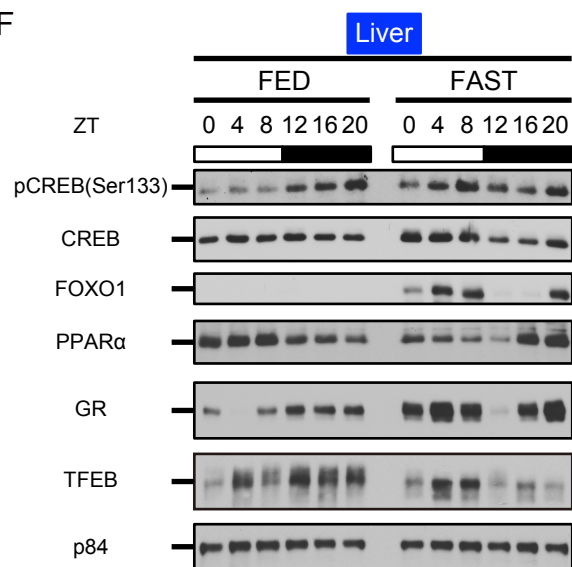
C



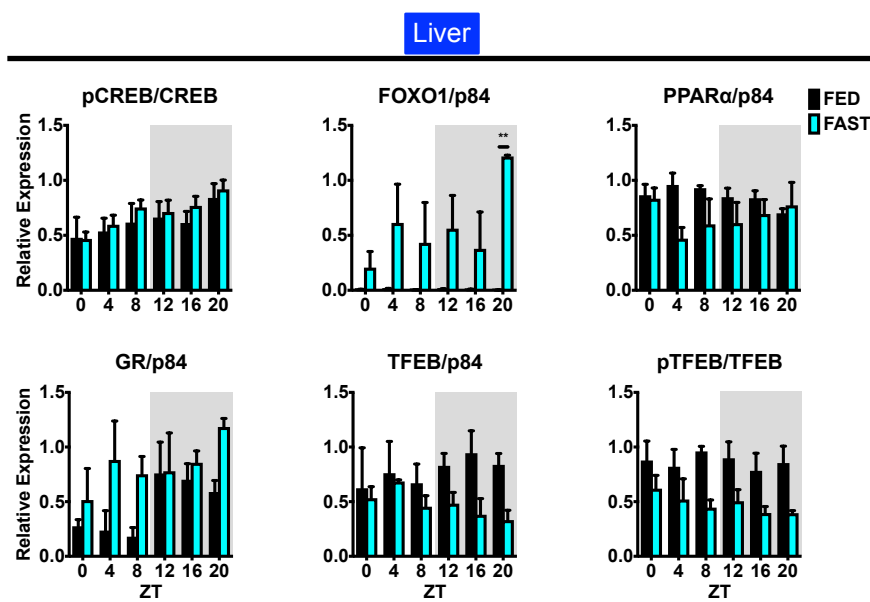
E



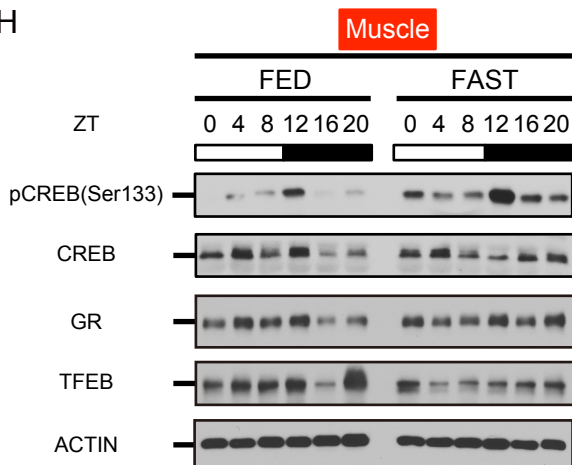
F



G



H



I

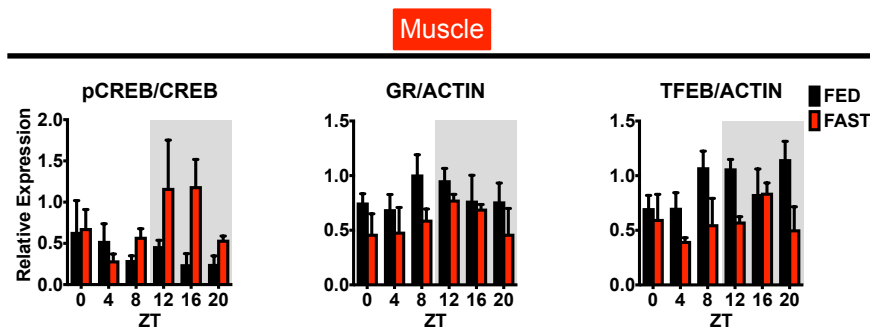


Figure S4. Differential gene regulation by the clock and fasting sensing pathways in the liver and skeletal muscle. Related to Figures 3 and 4.

(A) Representative immunoblots of hepatic SIRT1 and α -TUBULIN in whole cell lysates from FED and FAST mice over the circadian cycle. (B and C) Gene expression profiles of hepatic *Creb1*, *Nr3c1* (*GR*), *Tfeb*, and muscle *Creb1* measured by RNA-seq. Transcript levels were presented as mean + SEM (n=3 biological replicates per time point per group). ZT0 is double plotted for visualization. (D and E) Gene expression profiles of hepatic *Ppara* and *Foxo1*, and muscle *Ppard*, *Foxo1*, *Nr3c1* (*GR*), and *Tfeb* measured by RT-qPCR. Transcript levels were normalized to 18S ribosomal RNA and presented as mean + SEM (n=5 biological replicates per time point per group). ZT0 is double plotted for visualization. (F) Representative immunoblots and of hepatic phospho-CREB (pCREB), CREB, FOXO1, PPAR α , GR, TFEB, and p84 in nuclear extracts from FED and FAST mice. (G) Quantitation of the blot band density of the hepatic proteins presented as mean + SEM (n=3 biological replicates per time point per group). ** p < 0.01 by two-way ANOVA with Bonferroni post-hoc tests. The upper band density of hepatic TFEB was quantitated as phospho-TFEB (pTFEB). (H) Representative immunoblots of muscle pCREB, CREB, GR, TFEB, and ACTIN in whole cell lysates from FED and FAST mice. (I) Quantitation of the blot band density of the muscle proteins presented as mean + SEM (n=3 biological replicates per time point per group).

Figure S5

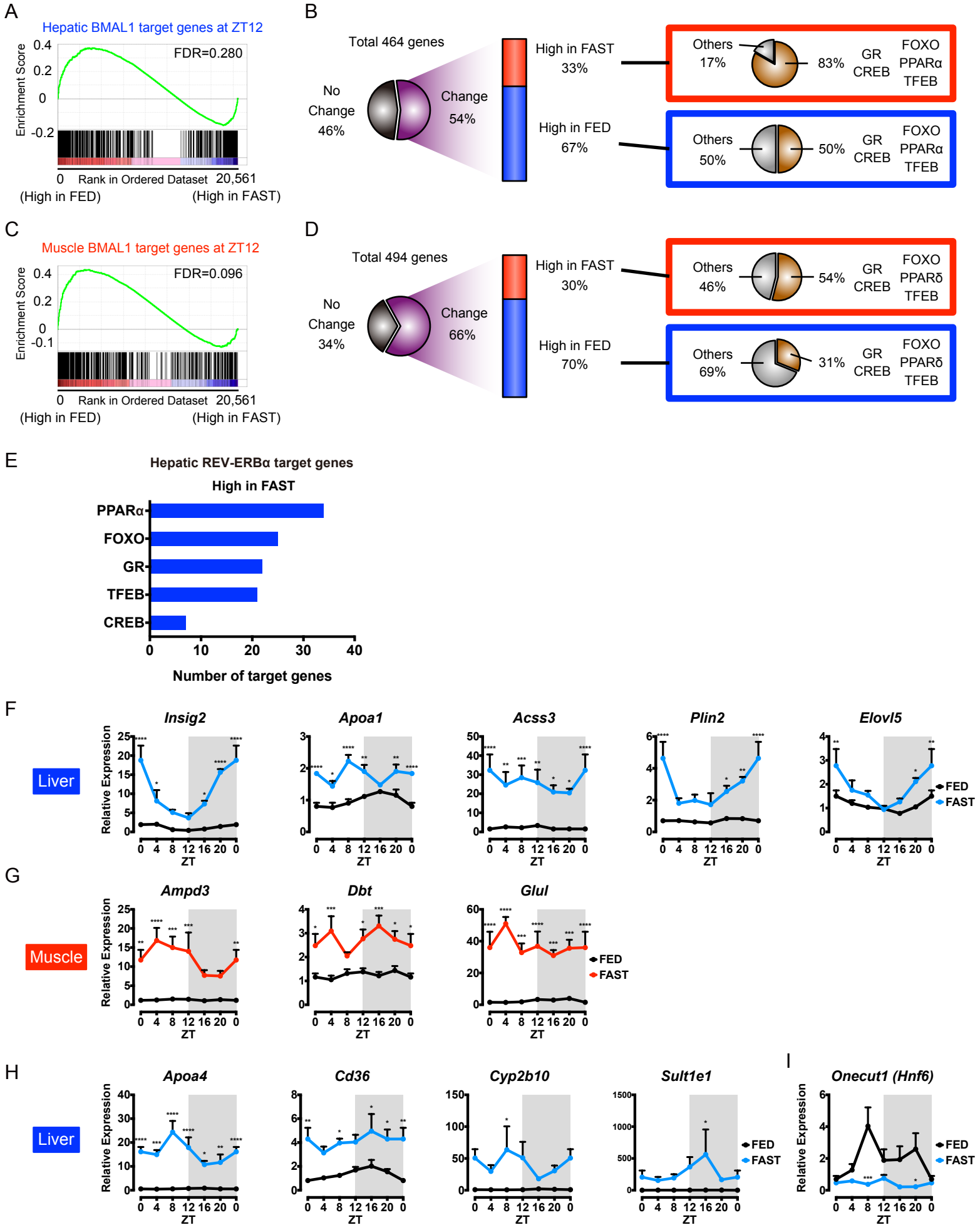


Figure S5. Temporal pattern of differential gene regulation by BMAL1 and REV-ERB α under fasting. Related to Figure 4.

(A) Gene set enrichment analysis (GSEA) for hepatic BMAL1 target genes at ZT12 enriched in FED. (B) Differentially expressed BMAL1 target genes in the liver at ZT12 illustrating fasting-sensitive TF coordinated regulation. (C) GSEA for muscle BMAL1 target genes at ZT12 enriched in FED. (D) Differentially expressed BMAL1 target genes in the muscle at ZT12 illustrating fasting-sensitive TF coordinated regulation. Gene sets with false discovery rate (FDR) < 0.25 are considered significantly enriched. (E) The numbers of hepatic GR, CREB, FOXO, TFEB, and PPAR α target genes among the hepatic REV-ERB α target genes expressed significantly higher in FAST mice. (F) Gene expression profiles of hepatic REV-ERB α targets by RT-qPCR of FED and FAST mice. (G) Gene expression profiles of muscle REV-ERB α /HDAC3 targets by RT-qPCR of FED and FAST mice. (H) Gene expression profiles of hepatic HNF6/REV-ERB α targets by RT-qPCR of FED and FAST mice. (I) Gene expression profile of hepatic *Onecut1* (*Hnf6*) by RT-qPCR of FED and FAST mice. Transcript levels were measured by RT-qPCR, normalized to 18S ribosomal RNA, and presented as mean + SEM (n=5 biological replicates per time point per group). ZT0 is double plotted for visualization. * p < 0.05, ** p < 0.01, *** p < 0.001, and **** p < 0.0001 by two-way ANOVA with Bonferroni post-hoc tests.

Figure S6

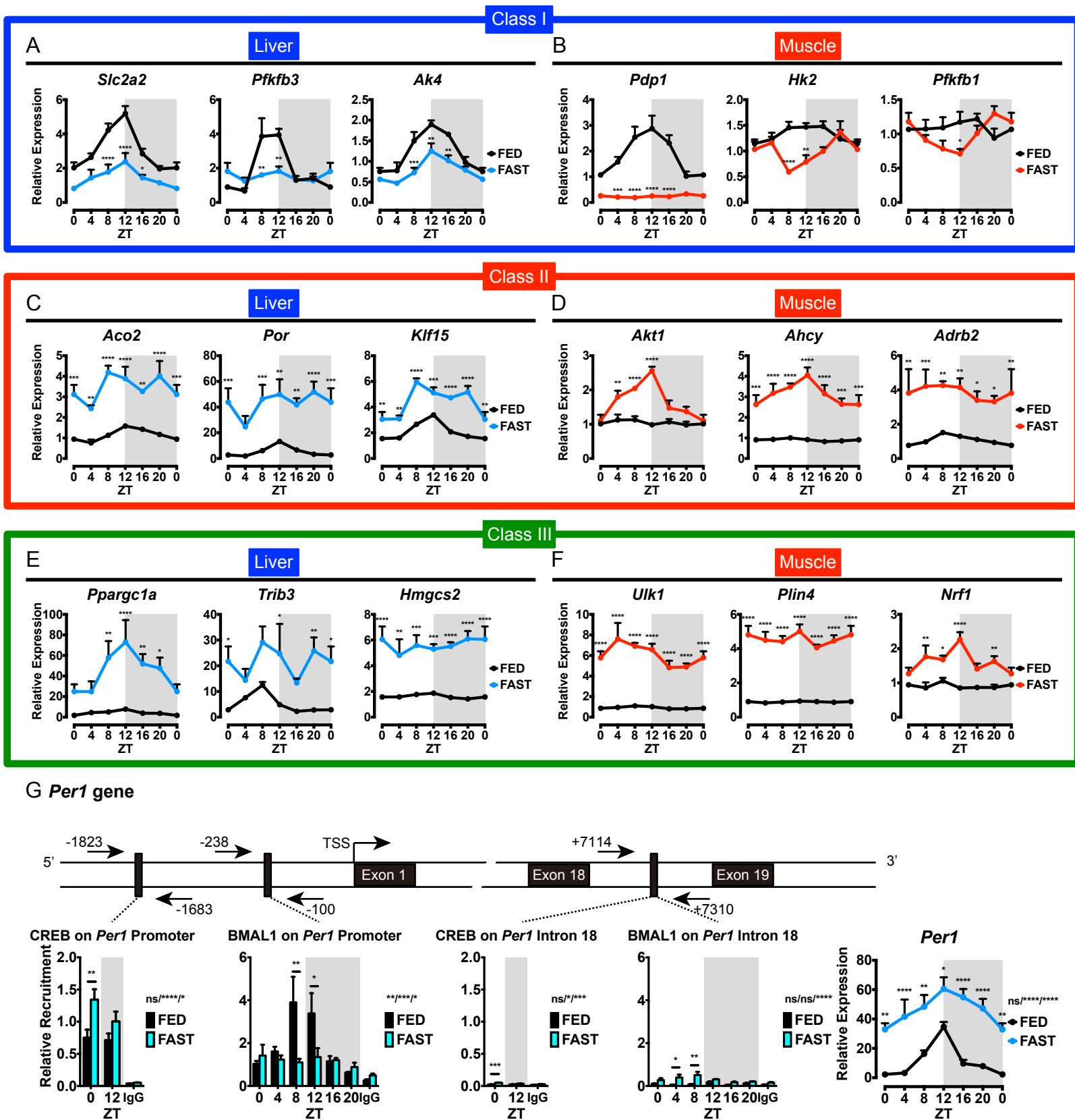


Figure S6. Differential gene regulation by clock and fasting responsive TFs. Related to Figure 5.

(A and B) Representative gene expression profiles of hepatic and muscle BMAL1 target genes repressed by fasting (Class I). (C and D) Representative gene expression profiles of hepatic and muscle BMAL1 target genes induced by fasting (Class II). (E and F) Representative gene expression profiles of hepatic and muscle fasting-induced genes of non-BMAL1 targets (Class III). Transcript levels were normalized to 18S ribosomal RNA and presented as mean + SEM (n=5 biological replicates per time point per group). ZT0 is double plotted for visualization. * p < 0.05, ** p < 0.01, *** p < 0.001, and **** p < 0.0001 by two-way ANOVA with Bonferroni post-hoc tests. (G) Chromatin immunoprecipitation in liver for BMAL1, CREB, or IgG followed by RT-qPCR specific for *Per1* gene. Data are presented as mean + SEM (n=3~4 biological replicates per time point per group). Diagram above shows schematic representation of *Per1* gene illustrating regions of amplification by primers designed for analysis (arrows). TSS denotes transcription start site. *Per1* gene expression profile is also shown next to CHIP-qPCR data for visualization. Transcript levels were normalized to 18S ribosomal RNA and presented as mean + SEM (n=5 biological replicates per time point per group). ZT0 is double plotted for visualization. * p < 0.05, ** p < 0.01, *** p < 0.001, and **** p < 0.0001 by two-way ANOVA (interaction/time/group) with Bonferroni post-hoc tests.

Figure S7

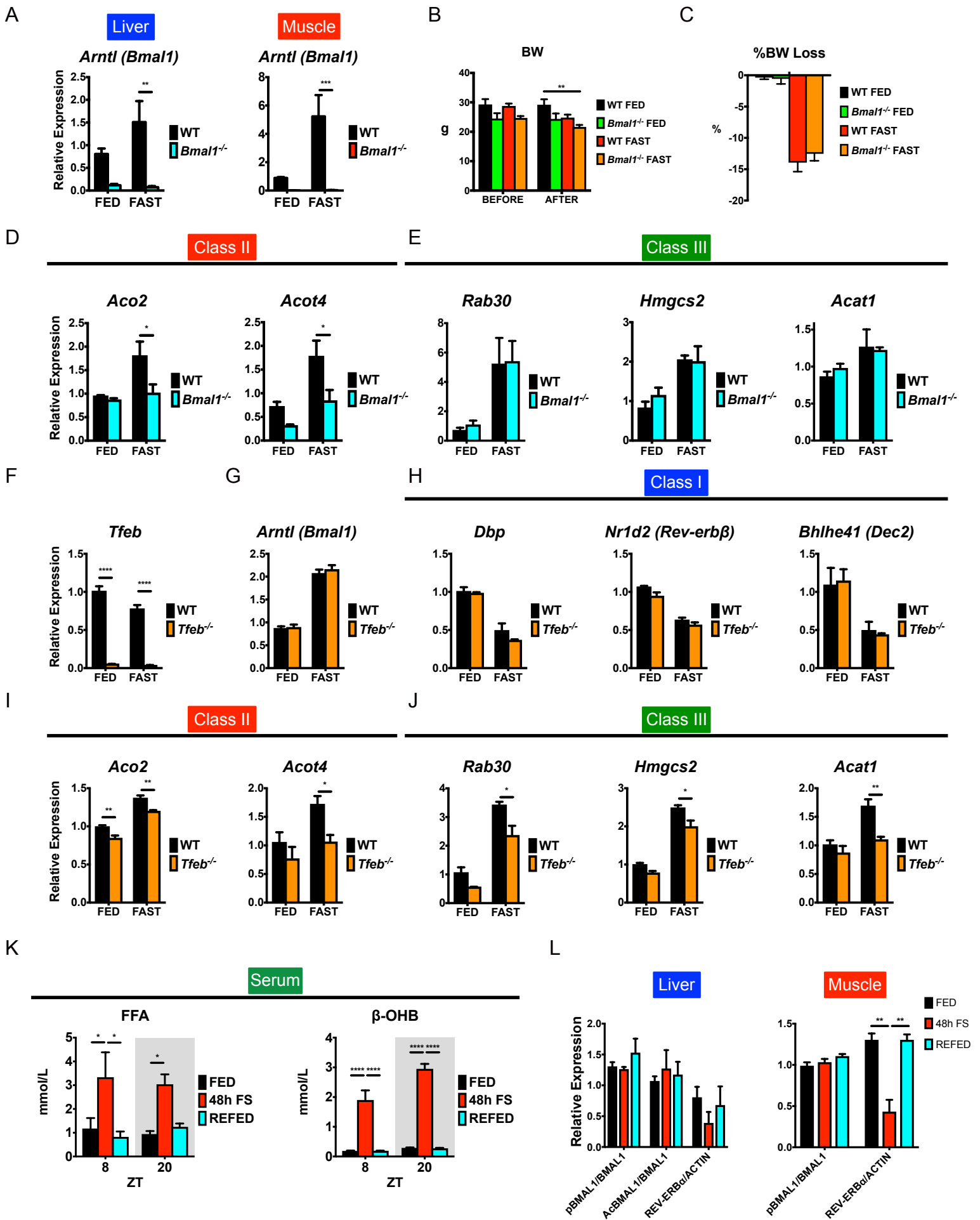


Figure S7. Differential gene regulation by clock and fasting responsive TFs, and temporal response to fasting. Related to Figures 6 and 7.

(A) Hepatic and muscle gene expression of *Arntl* (*Bmal1*) in WT and *Bmal1*^{-/-} mice at ZT8. Transcript levels were normalized to 18S ribosomal RNA and presented as mean + SEM (n=4~5 biological replicates per genotype per group). (B) Body weight of WT and *Bmal1*^{-/-} mice before and after 24-hr fasting. Data are shown as mean + SEM (n=4~5 biological replicates per genotype per group). (C) % body weight loss after 24-hr fasting at ZT8. Data are shown as mean - SEM (n=4~5 biological replicates per genotype per group). (D) Representative gene expression profiles of hepatic BMAL1 target genes induced by fasting (Class II) in WT and *Bmal1*^{-/-} mice at ZT8. (E) Representative gene expression profiles of hepatic fasting-induced genes of non-BMAL1 targets (Class III) in WT and *Bmal1*^{-/-} mice at ZT8. Data are shown as mean + SEM (n=4~5 biological replicates per genotype per group). (F and G) Hepatic gene expression of *Tfeb* and *Arntl* (*Bmal1*) in WT and *Tfeb* LiKO (*Tfeb*^{-/-}) mice at ZT8. (H) Representative gene expression profiles of hepatic BMAL1 target genes repressed by fasting (Class I) in WT and *Tfeb*^{-/-} mice at ZT8. (I) Representative gene expression profiles of hepatic BMAL1 and TFEB target genes induced by fasting (Class II) in WT and *Tfeb*^{-/-} mice at ZT8. (J) Representative gene expression profiles of hepatic TFEB-target, non-BMAL1 target genes induced by fasting (Class III) in WT and *Tfeb*^{-/-} mice at ZT8. Data are shown as mean + SEM (n=3~5 biological replicates per genotype per group). (K) Serum free fatty acid (FFA) and β -OHB levels from mice under *ad libitum* fed (FED), 48-hr fasting (48h FS), and 24-hr fasting with 24-hr refeeding (REFED) conditions. Data are shown as mean + SEM (n=3 biological replicates per time point per group). (L) Quantitation of the blot band density presented as mean + SEM (n=3 biological replicates per group). *p < 0.05, **p < 0.01, ***p < 0.001, and ****p < 0.0001 by two-way ANOVA with Bonferroni post-hoc tests.